Inorg. Chem. **2007**, *46*, 8349–8361

Oxidation of Guanine in Double-Stranded DNA by $[Ru(bpy)_2dppz]Cl_2$ in Cationic Reverse Micelles

Sarah E. Evans, Armine Grigoryan, and Veronika A. Szalai*

Department of Chemistry & Biochemistry, University of Maryland, Baltimore County, 1000 Hilltop Circle, Baltimore Maryland 21250

Received January 15, 2007

DNA oxidation has been investigated in the medium of cationic reverse micelles (RMs). The oxidative chemistry is photochemically initiated using the DNA intercalator bis(bipyridine)dipyridophenazine ruthenium(II) chloride ($[Ru(bpy)_2dppz]Cl_2$) bound to duplex DNA in the RMs. High-resolution polyacrylamide gel electrophoresis (PAGE) is used to reveal and quantify guanine (G) oxidation products, including 8-oxo-7,8-dihydroguanine (8OG). In buffer solution, the addition of the oxidative quenchers potassium ferricyanide or pentaamminechlorocobalt(III) dichloride leads to an increase in the amount of piperidine-labile G oxidation products generated via one-electron oxidation. In RMs, however, the yield of oxidatively generated damage is attenuated. With or without ferricyanide quencher in the RMs, the yield of oxidatively generated products is approximately the same. Inclusion of the cationic quencher $[CoCl(NH_3)_5]^{2+}$ in the RMs increases the amount of oxidation products generated but not to the extent that it does in buffer solution. Under anaerobic conditions, all of the samples in RMs, with or without added oxidative quenchers, show decreased levels of piperidine-labile oxidation products, suggesting that the primary oxidant in RMs is singlet oxygen. G oxidation is enhanced in D_2O and deuterated heptane and is diminished in the presence of sodium azide in RMs, also supporting $^1O_2$ as the main G oxidant in RMs. Isotopic labeling experiments show that the oxygen atom in 8OG produced in RMs is not from water. The observed change in the G oxidation mechanism from a one-electron process in buffer to mostly $^1O_2$ in RMs illustrates the importance of both DNA structure and DNA environment on the chemistry of G oxidation.

Introduction

DNA oxidation has been implicated in aging and cancer in cells and thus has been studied extensively using a variety of oxidants and reaction conditions.[1] Photosensitizers, including organic compounds and transition-metal complexes, can initiate damage in the DNA backbone or at DNA bases via several mechanisms, after exposure to light.[2] In particular, the fortuitous match between the redox potential of guanine (G) in DNA and ruthenium polypyridyl(III) complexes has led to the use of the latter as one-electron DNA oxidants, even though ruthenium complexes are not physiologically available.[1,3] A principal advantage of using ruthenium polypyridyl complexes to effect one-electron oxidation of G residues in DNA is that their DNA oxidation chemistry can be photoinitiated in the presence of a suitable quencher, as demonstrated by Barton's group (Scheme 1).[4] We use these compounds because their DNA oxidation chemistry has been well-documented and because their interaction with DNA can be modified easily by changes to the polypyridyl ligands.[5−9]

Most work probing DNA oxidation chemistry is typically carried out in aqueous buffered solution.[10] These studies have provided significant insight into the types of lesions that are

* To whom correspondence should be addressed. E-mail: vszalai@umbc.edu.

(1) Burrows, C. J.; Muller, J. G. *Chem. Rev.* **1998**, *98*, 1109.
(2) Armitage, B. *Chem. Rev.* **1998**, *98*, 1171.
(3) Steenken, S. *Chem. Rev.* **1989**, *89*, 503. Steenken, S.; Jovanovic, S. V. *J. Am. Chem. Soc.* **1997**, *119*, 617.
(4) Stemp, E. D.; Arkin, M. R.; Barton, J. K. *J. Am. Chem. Soc.* **1997**, *119*, 2921.
(5) Barton, J. K. *J. Biomol. Struct. Dyn.* **1983**, *1*, 621. Kumar, C. V.; Barton, J. K.; Turro, N. J. *J. Am. Chem. Soc.* **1985**, *107*, 5518. Lincoln, P.; Broo, A.; Norden, B. *J. Am. Chem. Soc.* **1996**, *118*, 2644. Ruba, E.; Hart, J. R.; Barton, J. K. *Inorg. Chem.* **2004**, *43*, 4570. Satyanarayana, S.; Dabrowiak, J. C.; Chaires, J. B. *Biochemistry* **1993**, *32*, 2573.
(6) Friedman, A. E.; Chambron, J.; Sauvage, J.; Turro, N. J.; Barton, J. K. *J. Am. Chem. Soc.* **1990**, *112*, 4960.
(7) Friedman, A. E.; Kumar, C. V.; Turro, N. J.; Barton, J. K. *Nucleic Acids Res.* **1991**, *19*, 2595.
(8) Haq, I.; Lincoln, P.; Suh, D.; Norden, B.; Chowdhry, B. Z.; Chaires, J. B. *J. Am. Chem. Soc.* **1995**, *117*, 4788.
(9) Chouai, A.; Wicke, S. E.; Turro, C.; Basca, J.; Dunbar, K. R.; Wang, D.; Thummel, R. P. *Inorg. Chem.* **2005**, *44*, 5996.

10.1021/ic0700708 CCC: $37.00
Published on Web 09/05/2007

Scheme 1. Photochemical Generation of Ru^{3+} and Its Subsequent Reaction with DNA

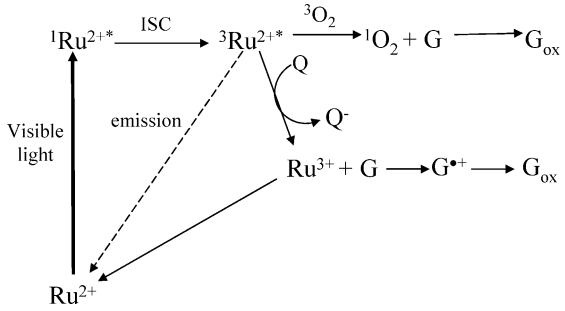

the most mutagenic and/or carcinogenic by elucidating oxidation mechanisms in dilute solution,[11] incorporating the oxidation products into DNA,[12] and testing the ability of replicative and repair enzymes to function using this damaged DNA.[13] However, the interiors of cells contain a high concentration of biomolecules,[14] and DNA is in a condensed state.[15] Thus, dilute solution measurements, while providing detailed mechanistic information, might not be representative of cellular DNA oxidation. On the other hand, mechanistic information about bond-making/breaking at the DNA is difficult to obtain in a cellular environment. Such information is important because of its potential impact on cellular processes such as transcription and repair.

Although monitoring oxidation chemistry in cells is the ideal, reverse micelles (RMs) offer a way to condense DNA in vitro.[16−19] RMs are formed by using surfactants with polar or charged head groups in an organic solvent with a small percentage of water. The headgroups come together to form water pools. Water-soluble molecules stay in the interior of the water pools, whereas hydrophobic molecules partition into the RM shell formed by the surfactant tails. The size of RMs is determined by the w_0 value, where $w_0 = [H_2O]/[\text{surfactant}]$, and this value has been correlated with the water pool size.[20,21] When incorporated in RMs, large-molecular-weight DNA adopts a different structure than that of DNA in buffer solution. For example, in RMs composed of a surfactant with an anionic headgroup, the DNA structure is similar to that found for "polymer-salt-induced" (psi)-DNA.[22] For our purposes, the photophysical properties of ruthenium polypyridyl complexes and their quenching processes have been studied extensively in RMs.[20,23] Our goal is to further reveal the effect of the DNA environment/structure on G oxidation chemistry, by using ruthenium polypyridyl complexes in conjunction with DNA entrapped in RMs.

Previously, we have reported on the reduced oxidation susceptibility of single- and double-stranded DNA encapsulated in anionic RMs and exposed to the simple electrostatic DNA-binder $Ru(bpy)_3^{3+}$.[24] In the work presented here, the chemistry of the DNA intercalator $Ru(bpy)_2dppz^{2+}$ with double-stranded DNA in cationic RMs is described. Our results indicate a change in the predominant mechanism of DNA oxidation by $Ru(bpy)_2dppz^{2+}$ when it is bound to DNA in RMs.

Experimental Section

Reagents: Racemic bis(2,2′-bipyridine)dipyridophenazine ruthenium(II) hexafluorophosphate ($[Ru(bpy)_2dppz](PF_6)_2$) was a gift from Dr. Rebecca Holmberg and Dr. H. Holden Thorp at the University of North Carolina at Chapel Hill. The chloride salt of $[Ru(bpy)_2dppz](PF_6)_2$ was generated by dissolving the complex in acetone and adding a concentrated solution of tetraethylammonium chloride in acetone. The extinction coefficient for $Ru(bpy)_2dppz^{2+}$ is 16 100 $M^{-1}cm^{-1}$ at 444 nm in water,[25] and the concentration of the racemic stock solution was determined spectrophotometrically using a Jasco V-560 dual beam UV−vis spectrophotometer. Water was deionized and polished using a Milli-Q Academic A10 water purification system (resistivity >18 mΩ and total organic content of <10 ppb). Solutions of 40% acrylamide/bis(acrylamide) in a 19:1 ratio were purchased from National Diagnostics (Atlanta, GA). Na_2IrCl_6 was from Alfa-Aesar (Ward Hill, MA). Tetramethylethylenediamine (TEMED), ammonium persulfate, mercaptoethanol, ethylenediamine tetraacetic acid disodium salt (Na_2EDTA), potassium ferricyanide ($K_3[Fe(CN)_6]$), sodium azide (NaN_3), D_2O (100% atom D), and *n*-heptane-d_{16} (99+ atom %D) were purchased from Acros (Morris Plains, NJ). Heptane, *n*-butanol, tris(hydroxymethyl)aminomethane (TRIS), boric acid, and urea were purchased from Fisher (Pittsburgh, PA). Piperidine and dimethylsulfate were purchased from Aldrich (Milwaukee, WI). Hexadecyl trimethylammonium bromide (CTAB) and nuclease *P*1 were purchased from Sigma (St. Louis, MO). Alkaline phosphatase was from Calbiochem (San Diego, CA). $H_2{}^{18}O$ (95% atom ^{18}O) was purchased from Isotec, a division of Sigma-Aldrich. Herring-testes DNA was purchased from Sigma and was selected because high molecular weight DNA previously has been shown to condense in RMs.[16,22] Oligonucleotides were purchased from either the W. M. Keck Facility (Yale University) or the Midland Oligonucleotide Company (Midland, TX). The concentrations of herring-testes DNA and oligonucleotides in water were determined spectrophotometrically. The extinction coefficient of herring-testes DNA in nucleotide phosphates is 6600 $M^{-1}cm^{-1}$.[26] Using the nearest-neighbor approximation,[27] the oligonucleotides' extinction coefficients were determined to be 222.7

(10) Delaney, S.; Pascaly, M.; Bhattacharya, P. K.; Han, K.; Barton, J. K. *Inorg. Chem.* **2002**, *41*, 1966.
(11) Cadet, J.; Berger, M.; Buchko, G. W.; Joshi, P. C.; Raoul, S.; Ravanat, J.-L. *J. Am. Chem. Soc.* **1994**, *116*, 7403. Ye, Y.; Muller, J. G.; Luo, W.; Mayne, C. L.; Shallop, A. J.; Jones, R. A.; Burrows, C. J. *J. Am. Chem. Soc.* **2003**, *125*, 13926. McCallum, J. E.; Kuniyoshi, C. Y.; Foote, C. S. *J. Am. Chem. Soc.* **2004**, *126*, 16777.
(12) Duarte, V.; Muller, J. G.; Burrows, C. J. *Nucleic Acids Res.* **1999**, *27*, 496.
(13) Duarte, V.; Gasparutto, D.; Jaquinod, M.; Ravanat, J.; Cadet, J. *Chem. Res. Toxicol.* **2001**, *14*, 46.
(14) Zimmerman, S. B.; Trach, S. O. *J. Mol. Biol.* **1991**, *222*, 599.
(15) Watanabe, K.; Iso, K. *Biochemistry* **1984**, *23*, 1376. Luger, K.; Mader, A. W.; Richmond, R. K.; Sargent, D. F.; Richmond, T. J. *Nature* **1997**, *389*, 251.
(16) Imre, V. E.; Luisi, P. L. *Biochem. Biophys. Res. Commun.* **1982**, *107*, 538. Luisi, P. L.; Giomini, M.; Pileni, M. P.; Robinson, B. H. *Biochim. Biophys. Acta* **1988**, *947*, 209.
(17) Braun, C. S.; Jas, G. S.; Choosakoonkriang, S.; Koe, G. S.; Smith, J. G.; Middaugh, C. R. *Biophys. J.* **2003**, *84*, 1114.
(18) Budker, V. G.; Slattum, P. M.; Monahan, S. D.; Wolff, J. A. *Biophys. J.* **2002**, *82*, 1570.
(19) Osfouri, S.; Stano, P.; Luisi, P. L. *J. Phys. Chem. B* **2005**, *109*, 19929.
(20) Atik, S. S.; Thomas, J. K. *J. Am. Chem. Soc.* **1981**, *103*, 4367.
(21) Atik, S. S.; Thomas, J. K. *J. Am. Chem. Soc.* **1981**, *103*, 3543. Maitra, A. *J. Phys. Chem.* **1984**, *88*.
(22) Pietrini, A. V.; Luisi, P. L. *Biochim. Biophys. Acta* **2002**, *1562*, 57.
(23) Atik, S. S.; Thomas, J. K. *J. Am. Chem. Soc.* **1981**, *103*, 7403.
(24) Evans, S. E.; Mon, S.; Singh, R.; Ryzhkov, L. R.; Szalai, V. A. *Inorg. Chem.* **2006**, *45*, 3124.
(25) Amouyal, E.; Homsi, A.; Chambron, J. C.; Sauvage, J. P. *J. Chem. Soc., Dalton Trans.* **1990**, *6*, 1841.
(26) Sigma-Aldrich, Technical Support.

$mM^{-1}cm^{-1}$ per strand for 5′-d[GATGAGAGTTAGTGATGAGTG]-3′ (**1**) and 190.2 $mM^{-1}cm^{-1}$ per strand for 5′-d[CACTCATCACTAACTCTCATC]-3′ (**2**). The sequence of the oligonucleotide with the GG step is 5′-d[GATGAGAGTTAGGTATGAGTG]-3′ (**3**), and its extinction coefficient is 223.5 $mM^{-1}cm^{-1}$. The complementary strand sequence is 5′-d[CACTCATACCTAACTCTCATC]-3′ (**4**), and its extinction coefficient is 190.8 $mM^{-1}cm^{-1}$. An oligonucleotide containing 8-oxo-7,8-dihydroguanine (8OG) with the sequence 5′-d[TATT(8OG)ATAT]-3′ was used as a standard for digestion and LC-MS experiments. CTAB stock solutions of 0.2 M and $w_0 = 10$ were prepared in a 90:10 heptane/butanol mixture[28] and passed through a Whatman 0.5 micron PTFE filter before use. Final samples were prepared by the addition of aqueous components to stock solutions of CTAB in heptane to give $w_0 = 20$ in all of the cases where w_0 is defined as $[H_2O]/[CTAB]$.

It is important to remember that RM solutions are microemulsions containing discrete water pools. At the water/surfactant ratio used in our work ($w_0 = 20$), the RM solutions contain approximately 800 μM water pools,[29] which is much higher than the concentration of either the $Ru(bpy)_2dppz^{2+}$ or the DNA. The concentration of $Ru(bpy)_2dppz^{2+}$ complexes per water pool is in part governed by the number of $Ru(bpy)_2dppz^{2+}$ molecules bound per DNA and the DNA duplex concentration. Thus, at the duplex concentrations used in our experiments, the effective concentration of $Ru(bpy)_2dppz^{2+}$ molecules in each water pool is very low.

Emission Spectroscopy. Emission spectra of samples containing $Ru(bpy)_2dppz^{2+}$ ($\lambda_{ex} = 444$ nm) were collected on either a Jobin-Yvon Fluoromax-2 fluorimeter or a Jobin-Yvon Fluorolog-3 fluorimeter. Emission spectra were collected from 500 to 800 nm with 2 nm increments, with an integration time of 0.5 s, and a slit width of 2 nm. Quenching studies of $Ru(bpy)_2dppz^{2+}$ emission with $Fe(CN)_6^{3-}$ or $[Co(NH)_5Cl]^{2+}$ were carried out in buffer solution and CTAB RMs ($w_0 = 20$) and in the presence of double-stranded herring-testes DNA or double-stranded 21-mer **1**:**2**. Double-stranded 21-mer **1**:**2** stock solutions were generated by adding an equimolar ratio of each strand in buffer solution, heating the solution for 5 min at 95 °C, and allowing the solution to come slowly to room temperature over 2−3 h. Emission spectra of $Ru(bpy)_2dppz^{2+}$ in buffer and CTAB RMs were collected in the presence of double-stranded 21-mer **1**:**2**. For samples prepared without O_2, solutions were frozen in liquid nitrogen and exposed to three freeze−pump−thaw cycles in a modified fluorescence cuvette under an atmosphere of N_2. The integrity of the RMs remains intact upon slow freezing in liquid N_2.[30] The modified cuvette has a side arm with a 50 mL round-bottomed flask and a high-vacuum stopcock for anaerobic sample preparation. All of the samples were prepared in triplicate, and the reported error is the standard deviation of the measurements.

Singlet oxygen emission experiments were performed on an Edinburgh Instruments FLS920 Spectrophotometer coupled to a NIR PMT capable of measuring $^1O_2$ emission at 1270 nm. The detection limit of the instrument for $^1O_2$ was determined using serial dilutions of buckminsterfullerene (C_{60}) in heptane (Supporting Information, Figure S1). RM samples containing 50 μM $Ru(bpy)_2dppz^{2+}$, 400 μM herring-testes DNA, 10 mM NaP_i, and $w_0 = 20$ were run with the same parameters used with C_{60} to observe $^1O_2$ emission.

Circular Dichroism (CD) Spectroscopy. Spectra were collected from 200−400 nm using a Jasco J-710 spectropolarimeter with the following parameters: sensitivity, 100 mdeg; data pitch, 0.5 nm; scanning mode, continuous; scanning speed, 200 nm/min; response, 1 s; bandwidth; 1 nm; and three accumulations. Spectra of double-stranded 21-mer **1**:**2** in buffer, and RMs were collected with and without $Ru(bpy)_2dppz^{2+}$. All of the samples were prepared in triplicate at the concentrations given in the figure legends. A background scan of matched solutions that did not contain double-stranded oligonucleotide was subtracted.

General Radiolabeling and Denaturing Polyacrylamide Gel Electrophoresis (PAGE). Oligonucleotides were piperidine-treated and gel-purified in a 20% polyacrylamide gel containing 7 M urea, according to standard procedures.[31] Purified **1** or **3** were radiolabeled with [γ-^{32}P]-ATP (10mCi/mL) using T4 polynucleotide kinase as previously described.[32] Denaturing PAGE was performed on 20% polyacrylamide gels with 7 M urea at 50 °C. Electrophoresis running buffer was 1X TBE prepared from a stock of 10X TBE with 0.89 M Tris, 20 mM EDTA, and 0.89 M boric acid, at pH 8.2−8.3. Gels were exposed to a phosphor screen for 1 h and scanned on an Amersham Biosciences Typhoon 9200. Quantification of band intensities was performed using *ImageQuaNT* software.

Oxidatively Generated Damage at Guanine (G) Sites. Double-stranded radiolabeled stock solutions were prepared by adding 1.1 equiv of complement (**2** or **4**) to 1 equiv of the G-containing oligonucleotide (**1** or **3**) in buffer solution. ^{32}P-radiolabeled oligonucleotide **1** (or **3**) was added, and the solution was heated at 95 °C for 5 min and allowed to cool to room temperature over 2−3 h. For RM samples, concentrations of all of the reactants were calculated on the basis of the total sample volume, whereas the buffer concentration was calculated on the basis of the volume of water in the sample. All of the RM samples were $w_0 = 20$. Samples were placed in capped vials with a path length of 4.3 mm, prior to illumination at room temperature using a 300 W Hg lamp (Oriel) with a UV cutoff filter. For RM samples without air, all of the sample components were mixed together except for the radioactive 21-mer duplex **1**:**2** (or **3**:**4**) solution. The samples in capped vials were subjected to three rounds of freeze−pump−thaw on a Schlenk line under N_2. A gas-tight syringe was used to add 2.5 μL of ^{32}P-labeled 21-mer duplex solution to the degassed RM samples immediately prior to illumination. On the basis of a 0.27 mM O_2 concentration in air-saturated water under normal atmospheric conditions, addition of this volume of duplex solution results in approximately 13 μM O_2 in the RM samples. After illumination, samples were ethanol-precipitated twice, piperidine treated (0.7 M piperidine, 90 °C for 30 min), and prepared for PAGE, as previously described.[32] Positions of Gs were determined by Maxam−Gilbert sequencing of ^{32}P-labeled **1**.[33]

Oxidation reactions were performed with $Ru(bpy)_2dppz^{2+}$ in the presence or absence of $Fe(CN)_6^{3-}$ in both buffer and RMs or with $[Co(NH_3)_5Cl]Cl_2$ in RMs. Samples contained 10 μM double-stranded 21-mer, 50 μM $Ru(bpy)_2dppz^{2+}$, and 10 mM NaP_i. Samples containing quencher had 500 μM or 1200 μM $Fe(CN)_6^{3-}$ or 100 or 250 μM $[Co(NH_3)_5Cl]Cl_2$. Samples were illuminated for 10, 30, or 60 min with $Fe(CN)_6^{3-}$ or for 30 min with $[Co(NH_3)_5Cl]^{2+}$. Average G cleavage ratios were calculated by dividing the

(27) Borer, P. N. *Handbook of Biochemistry and Molecular Biology*, 3rd ed.; CRC Press: Cleveland, OH, 1975.
(28) Kang, S. K.; McManus, H. J. D.; Liang, K.; Kevan, L. *J. Phys. Chem.* **1994**, *98*, 1044.
(29) Hubig, S. M.; Rodgers, M. A. J. *J. Phys. Chem.* **1990**, *94*, 1933.
(30) Baglioni, P.; Nakamura, H.; Kevan, L. *J. Phys. Chem.* **1991**, *95*, 3856. Nakamura, H.; Baglioni, P.; Kevan, L. *J. Phys. Chem.* **1991**, *95*, 1480. Jahn, W.; Strey, R. *J. Phys. Chem.* **1988**, *92*, 2294.
(31) Maniatis, T.; Fritsch, E. F.; Sambrook, J. *Molecular Cloning: A Laboratory Manual*, 2nd ed.; Cold Spring Harbor Press: Plainview, NY, 1989.
(32) Szalai, V. A.; Thorp, H. H. *J. Am. Chem. Soc.* **2000**, *122*, 4524.
(33) Sambrook, J.; Russell, D. W. *Molecular Cloning: A Laboratory Manual*, 3rd ed.; Cold Spring Harbor Laboratory Press: Cold Spring Harbor, New York, 2001; Vol. 2.

G band intensities by the parent band intensity. Errors given represent the standard deviation between the average G cleavage ratios for samples run in triplicate on each gel. To determine sequence selectivity in duplex **3**:**4**, which contains a GG step, the volume intensity of the 5′-G in the GG step (G5) was divided by the volume intensity of two other Gs in the sequence: the 3′-G in the GG step (G6) or another G more distant from the GG step (G3). Each gel was run at least three times.

To determine if $^1O_2$ is generated in our samples during illumination, RM samples were made with deuterated solvents or with azide, a quencher of $^1O_2$. These samples were illuminated, and the levels of oxidatively induced damage at G was determined by denaturing PAGE. For reactions performed in H_2O or D_2O, oligonucleotides **1** and **2** were combined in buffer solution in H_2O. This stock solution was divided in half, and the H_2O was removed from both aliquots by evaporation under reduced pressure. One of the pellets was resuspended in H_2O and the other in D_2O, and then the solutions were annealed (95 °C for 5 min, followed by slow cooling to room temperature over >2 h). The desired final concentrations of $Ru(bpy)_2dppz^{2+}$ and CTAB in the samples were generated by adding required volumes of stock solutions of each of these components prepared in 100% D_2O. All of these samples had final concentrations of 10 μM double-stranded 21-mer, 50 μM $Ru(bpy)_2dppz^{2+}$, and 10 mM NaP_i. Samples were illuminated in capped vials for 10, 30, or 60 min.

Oxidatively induced damage at G also was investigated in RM samples prepared with heptane or 100% d_{16}-heptane CTAB stock solutions (0.2 M). Samples contained 10 μM double-stranded 21-mer, 50 μM $Ru(bpy)_2dppz^{2+}$, and 10 mM NaP_i and were illuminated in capped vials for 10, 30, or 60 min.

Samples of RMs with or without added azide were prepared by adding azide dissolved in water to RM samples. These samples contained 10 μM double-stranded 21-mer, 50 μM $Ru(bpy)_2dppz^{2+}$, 10 mM NaP_i, and 500 μM azide. All of the samples were illuminated in capped vials for 10, 30, or 60 min.

Hexachloroiridate(IV) Treatment. To determine if 8OG is a product of G oxidation in the RMs, irradiated DNA was treated with $IrCl_6^{2-}$.[1] Samples with 10 μM double-stranded 21-mer, 50 μM $Ru(bpy)_2dppz^{2+}$, and 10 mM NaP_i in buffer or RMs were illuminated for 10, 25, and 60 min. Samples without added quencher were used for this experiment because the addition of an oxidative quencher to RMs does not significantly increase the yield of piperidine-labile products detected by PAGE and because the removal of O_2 decreases the damage yield. Following ethanol precipitation (2x), samples were treated with 100 μM $IrCl_6^{2-}$ for 60 min, and the reaction was quenched with HEPES/EDTA buffer. The samples were piperidine treated and analyzed by denaturing PAGE.

Isotopic Labeling. To determine the source of the oxygen atom in 8OG produced in RMs, samples were prepared with natural abundance H_2O or $H_2{}^{18}O$ (95% atom ^{18}O). Samples with 10 μM double-stranded 21-mer (**1**:**2**), 50 μM $Ru(bpy)_2dppz^{2+}$, and 10 mM NaP_i in bufffer or RMs were illuminated for 60 min and ethanol-precipitated twice. Samples then were exchanged into 10 mM cacodylate buffer using a microcon concentrator (3 kD MWC) prior to overnight digestion with nuclease *P*1 and alkaline phosphatase.[34] After digestion, the samples were filtered (microcon) to remove enzymes, and the filtrates were used for LC-MS experiments. The fragments were separated on a Waters 2695 Separations Unit, using a Phenomenex reversed-phase C18 Luna 5 μm column (100 Å pore size) with 5% acetonitrile/95% water (isocratic), and the masses were quantified using a Waters Micromass ZQ. The oligonucleotide 5′-d[TATT(8OG)ATAT-3′ was used as a standard for digestion and LC-MS experiments.

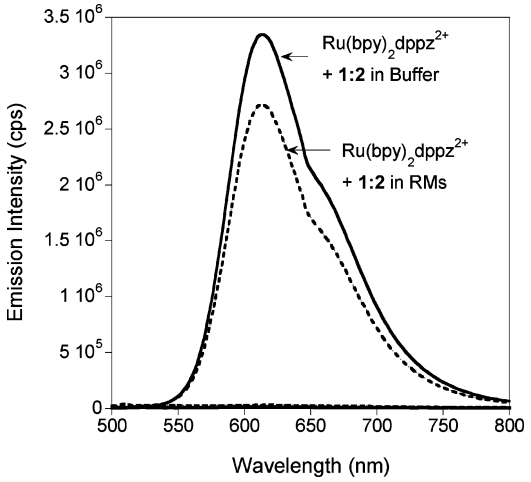

Figure 1. Emission spectra of $Ru(bpy)_2dppz^{2+}$ in the absence and presence of the 21-mer duplex oligonucleotide **1**:**2** in buffer (solid lines) and CTAB RMs (dashed lines). Concentrations: 50 μM $Ru(bpy)_2dppz^{2+}$, 10 μM 21-mer duplex **1**:**2**, and 10 mM NaP_i (pH 7). CTAB RMs are $w_0 = 20$.

Results and Discussion

Emission spectra of $Ru(bpy)_2dppz^{2+}$ are a diagnostic means to determine DNA binding.[6−8,10] In aqueous buffered solution, $Ru(bpy)_2dppz^{2+}$ does not display a steady-state emission spectrum, and the excited-state lifetime is very short (250 ps).[6,7,10,35,36] In the presence of double-stranded DNA, however, the steady-state emission intensity increases by a factor of 10^4 as a result of intercalation of the dppz ligand between the DNA base pairs.[6,35] In this environment, the excited-state lifetime of intercalated $Ru(bpy)_2dppz^{2+}$ increases to approximately 450 ns.[10] In CTAB RMs, an emission spectrum of $Ru(bpy)_2dppz^{2+}$ is observed only in the presence of double-stranded 21-mer **1**:**2** (Figure 1), indicating that the $Ru(bpy)_2dppz^{2+}$ complex is intercalated into the DNA. Compared to buffer solution containing the same double-stranded 21-mer and $Ru(bpy)_2dppz^{2+}$, the emission intensity of the $Ru(bpy)_2dppz^{2+}$ in CTAB RMs is decreased by about 20%.

Similar to the experiments with $Ru(bpy)_2dppz^{2+}$ in CTAB RMs, the emission intensity of $Ru(bpy)_3{}^{2+}$ was lower (by about 50%) in RMs composed of a negatively charged surfactant (AOT).[24] In that case, the emission maximum red-shifted by about 40 nm. We ascribed the decrease in emission intensity and shift of the emission maximum of $Ru(bpy)_3{}^{2+}$ to a significant change in the environment of the complex in the AOT RMs. In both this work and the previous work, buffer and RM samples had matched absorbances, so that the decrease in emission intensity is not due to different optical densities. Because a $Ru(bpy)_2dppz^{2+}$ emission spectrum is not observed in the absence of DNA, the decrease in emission intensity is not likely due to the complex binding

(34) Plum, G. E. *Current Protocols in Nucleic Acid Chemistry*; Wiley & Sons: New York, 2000, p 7.3.1.

(35) Hartshorn, R. M.; Barton, J. K. *J. Am. Chem. Soc.* **1992**, *114*, 5919.

(36) Arkin, M. R.; Stemp, E. D.; Holmlin, R. E.; Barton, J. K.; Hormann, A.; Olson, E. J.; Barbara, P. F. *Science* **1996**, *273*, 475.

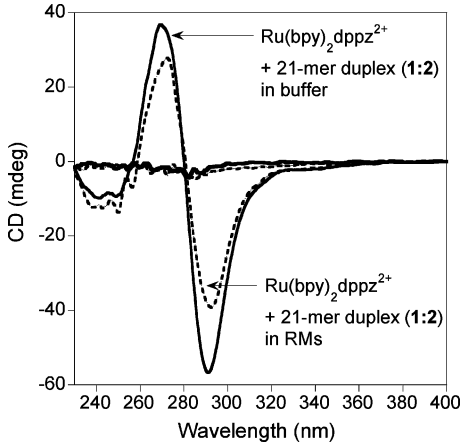

Figure 2. Circular dichroism spectra of $Ru(bpy)_2dppz^{2+}$ in the absence and presence of 21-mer duplex oligonucleotide **1**:**2** in buffer (solid lines) and CTAB RMs (dashed lines). Concentrations: 50 μM $Ru(bpy)_2dppz^{2+}$, 10 μM 21-mer oligonucleotide **1**:**2**, and 10 mM NaP_i (pH 7). CTAB RMs are $w_0 = 20$.

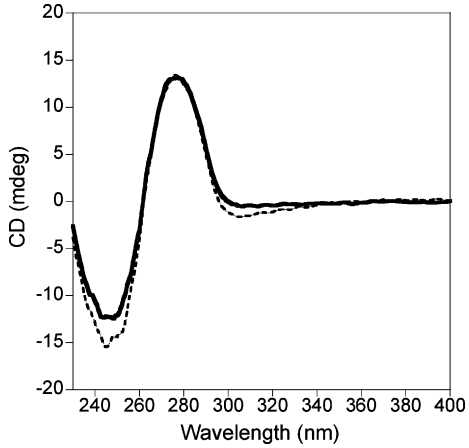

Figure 3. Circular dichroism spectra of 10 μM 21-mer duplex oligonucleotide **1**:**2** in buffer (solid line) and $w_0 = 20$ CTAB RMs (dashed line).

to the headgroups of the surfactants or because the complex is located in the organic component of the RM solution. $Ru(bpy)_2dppz^{2+}$ does display an emission spectrum in AOT RMs regardless of whether DNA is present, indicating that in those RMs the ruthenium complex binds to the surfactant headgroups.[24] In the CTAB RMs, the shape of the $Ru(bpy)_2dppz^{2+}$ emission spectrum does not differ from that in buffer solution. This result indicates that $Ru(bpy)_2dppz^{2+}$ is bound to DNA and/or localized in the water pool and not in the organic phase. If $Ru(bpy)_2dppz^{2+}$ were in the organic phase, its emission spectrum would be different.[37] The decreased emission intensity observed for $Ru(bpy)_2dppz^{2+}$ bound to DNA in the CTAB RMs either reflects a change in the excited-state lifetime(s) of $Ru(bpy)_2dppz^{2+}$ molecules bound to DNA or a decrease in the population of $Ru(bpy)_2dppz^{2+}$ molecules bound to DNA without a corresponding change in excited-state lifetime(s). Circular dichroism spectroscopy of $Ru(bpy)_2dppz^{2+}$ bound to DNA in CTAB RMs as described below supports the second explanation.

Circular dichroism spectroscopy offers a means to characterize the location of the $Ru(bpy)_2dppz^{2+}$ in relation to the DNA.[38] In a racemic mixture of both isomers of the complex, the CD spectrum is featureless (Figure 2). Upon intercalation of the $Ru(bpy)_2dppz^{2+}$ into DNA, an induced CD spectrum is observed because the bound molecules adopt the helicity of the duplex DNA.[39] In the presence of double-stranded 21-mer **1**:**2**, an induced CD spectrum is observed for $Ru(bpy)_2dppz^{2+}$ in both aqueous buffered solution and in CTAB RMs (Figure 2). The samples have matched absorbances, but the intensities of the positive and negative induced CD bands are decreased in the CTAB RMs by about 30%, which supports our assertion that fewer $Ru(bpy)_2dppz^{2+}$ molecules bind per DNA duplex when the DNA is in the CTAB RMs.

In addition to providing information about ligands bound to DNA, CD spectroscopy also is a useful probe of the structure of DNA within the reverse micelles.[22,40] For both herring-testes DNA and double-stranded 21-mer, CD spectra are similar in both buffer solution and CTAB RMs (Figure 3). These results are consistent with another study of DNA in CTAB RMs conducted at low ionic strength, indicating that the helicity of the DNA is unchanged by incorporation into these RMs.[18] However, even when the helicity of the DNA is conserved, molecular modeling of double-stranded DNA (10 bp) in liposomes prepared from DMPC (dimyristoylphosphatidylcholine) shows that the orientation of the bases can be distorted when the DNA is placed in the liposomes.[17] Thus, although the CD spectrum of the DNA might not change in reverse micelles, other characteristics dependent on base stacking might be affected. For example, the emission intensity of ethidium bromide intercalated into DNA decreases in neutral RMs as a result of a DNA structural change attributed to decreased flexibility.[18] Our emission and circular dichroism spectra of $Ru(bpy)_2dppz^{2+}$ with DNA in RMs are consistent with a model in which fewer $Ru(bpy)_2dppz^{2+}$ molecules bind per duplex, potentially as a result of a DNA structural change. A DNA structural change could decrease the number of bound $Ru(bpy)_2dppz^{2+}$ molecules, which explains why the emission intensity of $Ru(bpy)_2dppz^{2+}$ bound to DNA decreases when the DNA is in RMs and explains why the intensity of the induced $Ru(bpy)_2dppz^{2+}$ CD bands in the RMs also decreases.

To test our hypothesis that the changes in DNA structure induced by the RM solvent medium influence G oxidation chemistry, we performed oxidative quenching studies of $Ru(bpy)_2dppz^{2+}$ with $Fe(CN)_6^{3-}$ in CTAB RMs with double-stranded 21-mer **1**:**2** and generated Stern−Volmer plots, shown in Figure 4. Similar experiments were performed in buffer solution for direct comparison. It is important to remember that DNA must be included in these quenching experiments so that $Ru(bpy)_2dppz^{2+}$ displays an emission spectrum. In all of the cases, the addition of increasing

(37) Nair, R. B.; Cullum, B. M.; Murphy, C. J. *Inorg. Chem.* **1997**, *36*, 962.
(38) Yun, B. H.; Kim, J.-O.; Lee, B. W.; Lincoln, P.; Norden, B.; Kim, J.; Kim, S. K. *J. Phys. Chem. B* **2003**, *107*, 9858.
(39) Ardhammar, M.; Norden, B.; Kurucsev, T. In *Circular Dichroism: Principles and Applications*, 2nd ed.; Berova, N., Nakanishi, K., Woody, R. W., Eds.; Wiley & Sons: New York, NY, 2000; p 741.
(40) Brahms, J.; Mommaerts, W. F. *J. Mol. Biol.* **1964**, *10*, 73.

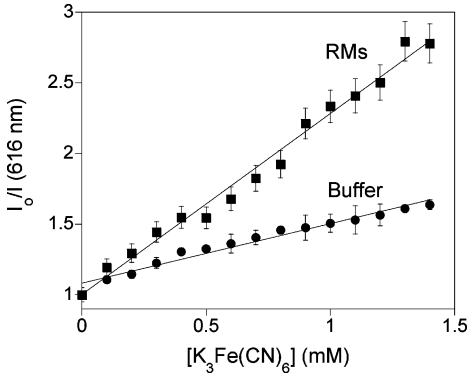

Figure 4. Stern−Volmer plot of $Ru(bpy)_2dppz^{2+}$ with double-stranded 21-mer **1**:**2** in buffer (circles) and RMs (squares). Concentrations: 50 μM $Ru(bpy)_2dppz^{2+}$, 10 μM 21-mer duplex **1**:**2**, 10 mM NaP_i (pH 7), and 0−1.4 mM $Fe(CN)_6^{3-}$.

Table 1. k_q Values Determined by Stern−Volmer Analysis of Oxidative Quenching of $Ru(bpy)_2dppz^{2+}$*

type of DNA	environment	$k_q \times 10^{-9}$ ($M^{-1}s^{-1}$)
herring testes	buffer	5.04 ± 0.22
	RM	4.23 ± 0.20
1:**2**	buffer	1.55 ± 0.10
	RM	4.98 ± 0.17

amounts of $Fe(CN)_6^{3-}$ decreases the emission intensity of the $Ru(bpy)_2dppz^{2+}$*, showing that the excited state is quenched. Because ferricyanide is an oxidative quencher of ruthenium(II) polypyridyl complexes,[41] we interpret these results to mean that $Ru(bpy)_2dppz^{3+}$ is generated in the CTAB RM system. Quenching rate constants (k_q) were determined using Stern−Volmer analysis (Table 1). The k_q value for $Ru(bpy)_2dppz^{2+}$* bound to the double-stranded 21-mer **1**:**2** is lower in buffer solution than in RM samples. We attribute this to the fact that the quencher and the $Ru(bpy)_2dppz^{2+}$* are in close proximity in the RMs, consistent with other work demonstrating that quenching increases in RMs.[20,42]

Other quenchers were tested in the CTAB RM system because the yield of the G radical cation generated by the related complex, $Ru(phen)_2dppz^{2+}$, depends on quencher identity.[43] The Stern−Volmer plot for $[Co(NH_3)_5Cl]^{2+}$ quenching of $Ru(bpy)_2dppz^{2+}$* bound to DNA in CTAB RMs indicates that this quencher is not as effective as $Fe(CN)_6^{3-}$ (Supporting Information, Figure S2). The lack of significant Ru^{2+}* quenching by $[Co(NH_3)_5Cl]^{2+}$ agrees with previously published work with $Ru(phen)_2dppz^{2+}$* in buffer solution.[4]

Oxidatively generated damage at G in a double-stranded 21-mer with (**3**:**4**) or without (**1**:**2**) a GG step was observed by high-resolution denaturing polyacrylamide gel electrophoresis (PAGE) and quantified by phosphorimagery. ^{32}P-radiolabeled samples containing $Ru(bpy)_2dppz^{2+}$ and $Fe(CN)_6^{3-}$ or $[Co(NH_3)_5Cl]^{2+}$ in RMs were illuminated to generate $Ru(bpy)_2dppz^{3+}$, which is a one-electron oxidant of G. Quantification of the gel band intensities reveals that, in CTAB RMs, the amount of damage with and without $Fe(CN)_6^{3-}$ is similar, indicating that this quencher is not necessary for DNA damage to occur (Figure 5). In contrast, in buffer solution, the amount of oxidatively generated damage at G increases upon the addition of $Fe(CN)_6^{3-}$ quencher (Figure 6). When $[Co(NH_3)_5Cl]^{2+}$ is used as the quencher in RMs, an increase in piperidine-labile products is observed relative to samples without added quencher or with ferricyanide (Figures 8, 9, and Table 2). This result is similar to that observed in buffer solution where the cobalt quencher produces the highest yields of the G radical when reacted with $Ru(phen)_2dppz^{2+}$* bound to duplex DNA.[43] In RMs, however, the enhancement is not as dramatic as in buffer solution (data not shown).[4]

On the basis of the previous observation that $Ru(bpy)_2dppz^{2+}$* bound to DNA generates $^1O_2$ in buffer solution,[10] it is possible that the principal oxidant generated in the CTAB RMs is $^1O_2$ instead of $Ru(bpy)_2dppz^{3+}$. Thus, a series of experiments were performed to determine if $^1O_2$ is the oxidant in the CTAB RM system. $^1O_2$ has a longer lifetime in D_2O ($\tau = 20$ μs in D_2O vs 2 μs in H_2O),[44,45] so performing oxidation reactions in D_2O should lead to an increase in oxidatively generated damage at G if $^1O_2$ is the oxidant.[9] In CTAB RMs containing duplex oligonucleotide and $Ru(bpy)_2dppz^{2+}$ prepared with D_2O, the level of oxidatively generated damage products of G is increased relative to similar samples prepared in H_2O (part A of Figure 7). Because samples prepared in RMs contain little water, another set of CTAB RM samples was prepared with d_{16}-heptane. In general, $^1O_2$ lifetimes increase in deuterated solvents,[45] and an increase in oxidatively generated damage should occur in CTAB RMs in d_{16}-heptane. When compared to samples prepared with heptane, the amount of oxidatively generated damage at G increased (part B of Figure 7).

Our results in deuterated solvents correlate well with other work on ruthenium complexes that produce $^1O_2$. For example, photoexcited $Ru(bpy)_3^{2+}$ and $Ru(phen)_3^{2+}$ in the presence of plasmid DNA show a cleavage enhancement of a factor of 2 in D_2O versus H_2O.[46] Also, ruthenium complexes of 1,12-diazaperylene derivatives show a significant increase in photocleavage of plasmid DNA in D_2O.[9] At 10 min illumination time for our D_2O and d_{16}-heptane RM samples, the cleavage is about double that observed in samples containing H_2O and heptane.

To further investigate the possibility that $^1O_2$ is the oxidant, RM samples with $Ru(bpy)_2dppz^{2+}$ were prepared and illuminated in the presence of sodium azide.[47,48] Azide is a quencher of $^1O_2$ ($k_q = 4 \times 10^8$ M^{-1} s^{-1} in H_2O),[49] and a decrease in the amount of oxidatively generated damage is expected in samples prepared with azide if $^1O_2$ is the

(41) Juris, A.; Gandolfi, M. T.; Manfrin, M. F.; Balzani, V. *J. Am. Chem. Soc.* **1976**, *98*, 1047.
(42) Atik, S. S.; Thomas, J. K. *J. Phys. Chem.* **1981**, *85*, 3921.
(43) Schiemann, O.; Turro, N. J.; Barton, J. K. *J. Phys. Chem. B* **2000**, *104*, 7214.
(44) Merkel, P. B.; Kearns, D. R. *J. Am. Chem. Soc.* **1972**, *94*, 1029.
(45) Merkel, P. B.; Nilsson, R.; Kearns, D. R. *J. Am. Chem. Soc.* **1971**, *94*, 1030.
(46) Fleisher, M. B.; Waterman, K. C.; Turro, N. J.; Barton, J. K. *Inorg. Chem.* **1986**, *25*, 3549.
(47) Hasty, N.; Merkel, P. B.; Radlick, P.; Kearns, D. R. *Tetrahedron Lett.* **1972**, *1*, 49.
(48) Hall, R. D.; Chignell, C. F. *Photochem. Photobiol.* **1987**, *45*, 459.
(49) Schweitzer, C.; Schmidt, R. *Chem. Rev.* **2003**, *103*, 1685.

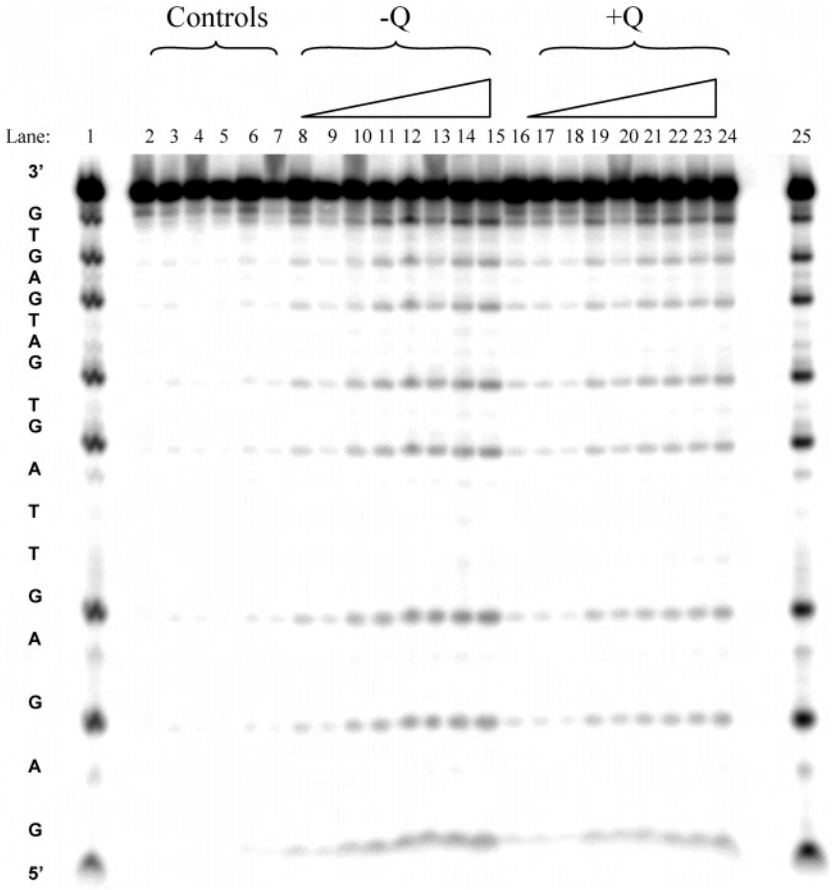

Figure 5. Phosphorimage of oxidatively generated damage at G of 10 μM 21-mer duplex **1**:**2** in CTAB RMs with 50 μM $Ru(bpy)_2dppz^{2+}$, 10 mM NaP_i, with or without 1.2 mM $Fe(CN)_6^{3-}$. Lanes 1 and 25 are Maxam−Gilbert sequencing lanes. Lanes 2−6 are controls: lane 2 is non-illuminated 21-mer duplex **1**:**2**, lane 3 is non-illuminated 21-mer duplex **1**:**2** with $Ru(bpy)_2dppz^{2+}$, lane 4 is non-illuminated 21-mer duplex **1**:**2** with $Ru(bpy)_2dppz^{2+}$ and $Fe(CN)_6^{3-}$, lane 5 is 21-mer duplex **1**:**2** illuminated for 60 min, and lane 6 is 21-mer duplex **1**:**2** illuminated in the presence of $Fe(CN)_6^{3-}$ for 60 min. Lanes 7−15 are samples without $Fe(CN)_6^{3-}$, and lanes 16−24 contain $Fe(CN)_6^{3-}$. Lanes 7−9 and 16−18 were illuminated for 10 min, lanes 10−12 and 19−21 were illuminated for 30 min, and lanes 13−15 and 22−24 were illuminated for 60 min.

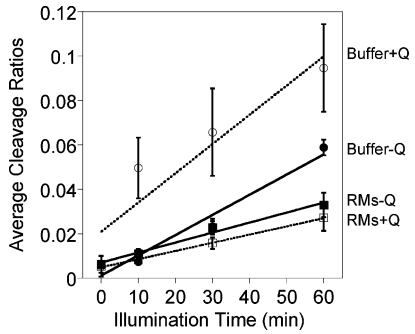

Figure 6. Plot of average cleavage ratios at G of 21-mer duplex oligonucleotide **1**:**2** in buffer or RMs, in the absence and presence of quencher. All of the samples contained 50 μM $Ru(bpy)_2dppz^{2+}$, 10 μM **1**:**2**, 10 mM NaP_i, and 1.2 mM $Fe(CN)_6^{3-}$ where indicated. Squares are the average cleavage ratios of Gs in the 21-mer duplex in CTAB RMs containing $Ru(bpy)_2dppz^{2+}$ without (RMs − Q, closed symbols) and with (RMs + Q, open symbols) $Fe(CN)_6^{3-}$. Circles are the average cleavage ratios of Gs in the 21-mer duplex in buffer without (buffer - Q, closed symbols) and with (buffer + Q, open symbols) quencher. See text for how average cleavage ratios were determined. A representative gel for the buffer samples is in the Supporting Information (Figure S4).

oxidant.[50] Emission studies of $Ru(bpy)_2dppz^{2+}$ with azide were first performed to ensure that azide does not quench $Ru(bpy)_2dppz^{2+}$*, which also would lead to a decrease in oxidatively generated damage. The emission characteristics of $Ru(bpy)_2dppz^{2+}$ were unaltered in the presence of azide (Supporting Information, Figure S3). Gel electophoresis experiments show a decrease in oxidatively generated damage products of G in double-stranded 21-mer **1**:**2** in the presence of azide when compared to similar samples prepared without azide (part C of Figure 7). This result also is consistent with $^1O_2$ being the oxidant in the CTAB RMs. In studies with the photosensitizer rose bengal, which is known to produce $^1O_2$, the amount of $^1O_2$ produced in the presence of azide is half of that produced in solutions without azide.[48] Similarly, we observe a 2-fold decrease in oxidatively generated damage at G in the presence of azide in RMs at the longest illumination times.

Finally, the yield of piperidine-labile products was quantified by PAGE for RM samples prepared with or without air (Figure 8). In all of the cases, there is a decrease in the amount of oxidatively generated damage when air is removed from the system. These data support a predominantly $^1O_2$-mediated G oxidation mechanism for $Ru(bpy)_2dppz^{2+}$ bound to DNA in RMs. One unexpected result is the decrease in piperidine-labile products observed with the $[Co(NH_3)_5Cl]^{2+}$ quencher. In aerated buffer solution, an increase in G cation

(50) Miyamoto, S.; Martinez, G. R.; Medeiros, M. H. G.; Di Mascio, P. *J. Am. Chem. Soc.* **2003**, *125*, 6172.

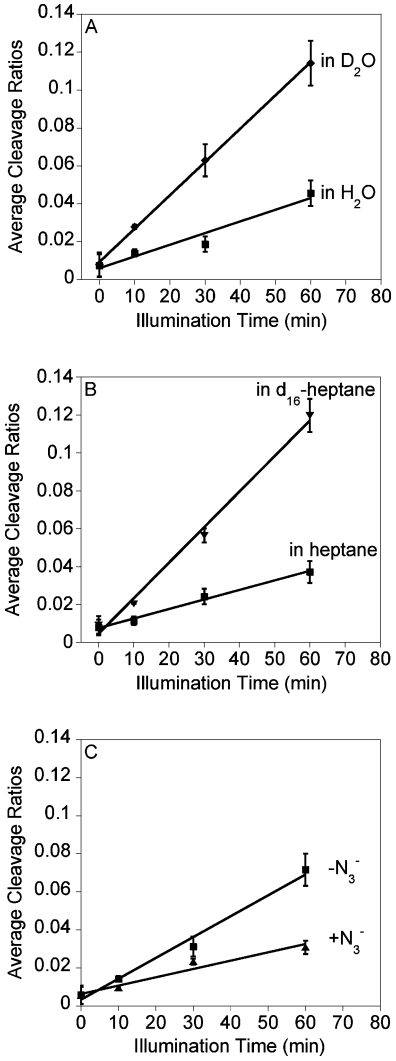

Figure 7. (A) Plot of average cleavage ratios of Gs in the 21-mer duplex **1**:**2** in CTAB RMs prepared with H_2O (squares) or D_2O (diamonds). (B) Plot of average cleavage ratios of Gs in 21-mer duplex **1**:**2** in CTAB RMs prepared with heptane (squares) or deuterated heptane (inverted triangles). (C) Plot of average cleavage ratios of Gs in 21-mer duplex **1**:**2** in CTAB RMs in the absence (squares) and presence (triangles) of NaN_3. All of the samples contained 50 μM $Ru(bpy)_2dppz^{2+}$ and 10 mM NaP_i and were $w_0 = 20$. Azide concentrations were 500 μM. Representative gels are given in the Supporting Information (Figure S5).

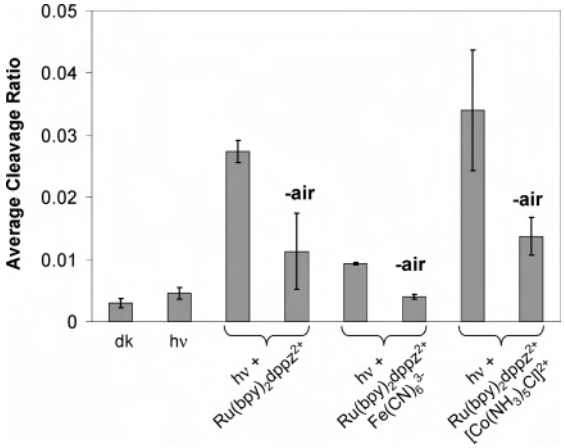

Figure 8. Quantification of average cleavage ratios of double-stranded 21-mer **1**:**2** in CTAB RMs in the presence of 50 μM $Ru(bpy)_2dppz^{2+}$ with $Fe(CN)_6^{3-}$ (1.2 mM) or $[Co(NH_3)_5Cl]^{2+}$ (250 μM) with and without air. Samples were illuminated for 30 min.

radical yield is observed for $Ru(phen)_2dppz^{2+}$ with $[Co(NH_3)_5Cl]^{2+}$ compared to other oxidative quenchers.[4] This observation was attributed to the lack of significant back-reaction between the reduced quencher and the G radical cation.[4] The dominant reaction of the G radical cation in duplex DNA is with water, generating the reducing G radical (II in Scheme 2). Oxidation of the reducing radical leads to the formation of 8OG, whereas reduction leads to 2,6-diamino-4-hydroxy-5-formamidopyrimidine (FapyG).[1] In oxygen-free aqueous solutions of DNA exposed to γ radiation, the relative yield of FapyG is higher than that of 8OG.[51] By analogy to other metal-based one-electron oxidants, 8OG oxidation by Ru^{3+} is expected to lead to spiroiminodihydantoin.[52] None of these pathways involves O_2, thus, we expected that removal of O_2 from the RMs would not affect the amount of piperidine-labile products generated by $Ru(bpy)_2dppz^{2+}$ with $[Co(NH_3)_5Cl]^{2+}$. The decreased quantity of piperidine-labile products detected by PAGE indicates that Ru^{3+} formation by $[Co(NH_3)_5Cl]^{2+}$ only partially contributes to the overall G oxidation chemistry in RMs with this quencher. With or without O_2, 8OG formed via the G radical cation can react with a second equivalent of Ru^{3+} to form piperidine-labile products. However, in the presence of O_2, 8OG also can react with $^1O_2$, generated by photosensitization of O_2 by Ru^{2+}*. $[Co(NH_3)_5Cl]^{2+}$ has a low k_q for Ru^{2+}*, which translates into a large concentration of Ru^{2+} excited states available to generate $^1O_2$. As a result, the amount of piperidine-labile products detected from the reaction of $Ru(bpy)_2dppz^{2+}$ with $[Co(NH_3)_5Cl]^{2+}$ in the presence of air is a sum of products from the O_2-independent and O_2-dependent pathways.

Although it has been demonstrated previously that the $Ru(bpy)_2dppz^{2+}$ excited state does not oxidize Gs in DNA directly,[10] it is important to establish that this mechanism does not operate in RMs. There are two principal mechanisms through which photoactive complexes can oxidize Gs.[1] The Type I pathway involves direct oxidation of G by the excited state of the photoactive complex, in our case $Ru(bpy)_2dppz^{2+}$*. Type II G oxidation is an indirect mechanism involving the generation of $^1O_2$, produced by the reaction of $^3O_2$ with the photosensitizer excited state. To differentiate a Type I from a Type II mechanism, we performed experiments in the presence or absence of air with a duplex oligonucleotide containing a GG step (**3**:**4**). The 5′-G in the GG step is the major site of oxidatively generated lesions if a Type I mechanism contributes to the oxidation chemistry. No sequence selectivity is observed if a Type II mechanism predominates.[1] We observe that there is only a small selectivity of the 5′-G (G5) in the GG step over other Gs in the sequence and that this selectivity diminishes or disappears when O_2 is removed (Figure 9 and Table 2). These results

(51) Douki, T.; Martini, R.; Ravanat, J.; Turesky, R.; Cadet, J. *Carcinogenesis* **1997**, *18*, 2385.
(52) Luo, W.; Muller, J. G.; Rachlin, E. M.; Burrows, C. J. *Org. Lett.* **2000**, *2*, 613. Luo, W.; Muller, J. G.; Rachlin, E. M.; Burrows, C. J. *Chem. Res. Toxicol.* **2001**, *14*, 927.

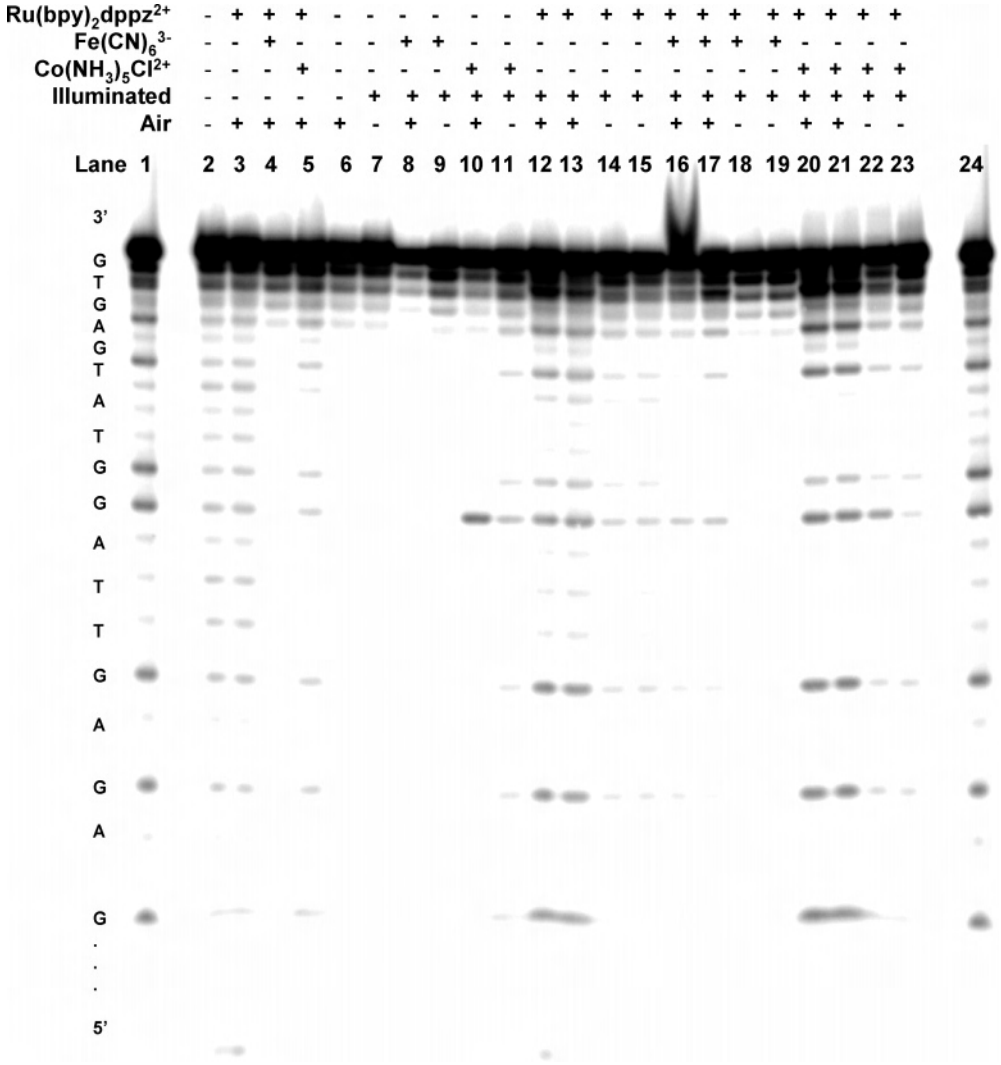

Figure 9. Phosphorimage of oxidatively generated damage at G with and without O_2 of 10 μM double-stranded 21-mer containing a GG step (**3**:**4**) in CTAB RMs with 50 μM $Ru(bpy)_2dppz^{2+}$, 10 mM NaP_i, with or without the quenchers $Fe(CN)_3^{6-}$ (1.2 mM) or $[Co(NH_3)_5Cl]^{2+}$ (100 μM). Lanes 1 and 24 are Maxam−Gilbert sequencing lanes. Lanes 2−11 are controls: lane 2 is non-illuminated **3**:**4**, lane 3 is non-illuminated **3**:**4** with $Ru(bpy)_2dppz^{2+}$, lane 4 is non-illuminated **3**:**4** with $Ru(bpy)_2dppz^{2+}$ with $Fe(CN)_6^{3-}$, lane 5 is non-illuminated **3**:**4** with $Ru(bpy)_2dppz^{2+}$ with $[Co(NH_3)_5Cl]^{2+}$, lanes 6 and 7 are **3**:**4** illuminated for 30 min, lanes 8 and 9 are **3**:**4** illuminated for 30 min in the presence of $Fe(CN)_6^{3-}$, and lanes 10 and 11 are **3**:**4** illuminated with $[Co(NH_3)_5Cl]^{2+}$ for 30 min. Lanes 7, 9, and 11 are without O_2. Lanes 12−15 contain **3**:**4** with $Ru(bpy)_2dppz^{2+}$, lanes 16−19 contain **3**:**4** with $Ru(bpy)_2dppz^{2+}$ and $Fe(CN)_6^{3-}$, and lanes 20−23 contain **3**:**4** with $Ru(bpy)_2dppz^{2+}$ and $[Co(NH_3)_5Cl]^{2+}$. All of the samples in lanes 12−23 were illuminated for 30 min and lanes 14, 15, 18, 19, 22, and 23 were without O_2.

Table 2. Band Volume Intensity Ratios of the 5′-G in the GG Step (G5) Relative to Other Gs in the Sequence (G6 or G3) of Duplex **3**:**4**

RM sample	G5/G6	G5/G3
$Ru(bpy)_2dppz^{2+}$	1.48 ± 0.02	1.25 ± 0.06
$Ru(bpy)_2dppz^{2+}$ − air	1.11 ± 0.02	1.28 ± 0.06
$Ru(bpy)_2dppz^{2+}$ + $Fe(CN)_6^{3-}$	1.83 ± 0.16	1.61 ± 0.11
$Ru(bpy)_2dppz^{2+}$ + $Fe(CN)_6^{3-}$ − air	1.13 ± 0.04	1.59 ± 0.12
$Ru(bpy)_2dppz^{2+}$ + $[Co(NH_3)_5Cl]^{2+}$	1.59 ± 0.06	0.91 ± 0.02
$Ru(bpy)_2dppz^{2+}$ + $[Co(NH_3)_5Cl]^{2+}$ − air	1.38 ± 0.52	1.33 ± 0.50

again indicate that a Type II mechanism is the main pathway of G oxidation in RMs, even in the presence of oxidative quenchers. The selectivity of the 5′-G in a GG step using $Ru(phen)_2dppz^{2+}$ and $Co(NH_3)_5Cl^{2+}$ in buffer solution is much greater[4] than the maximum ratio of approximately 2, observed in RMs with this quencher (Table 2). Further, the decrease in piperidine-labile lesions detected by PAGE for DNA illuminated in RMs containing azide also rules out a Type I mechanism. If $Ru(bpy)_2dppz^{2+}$* oxidizes Gs directly, the amount of piperidine-labile lesions detected by PAGE would be constant in the presence of azide because azide does not quench $Ru(bpy)_2dppz^{2+}$* (Supporting Information, Figure S3). We observe the opposite effect, which indicates that $Ru(bpy)_2dppz^{2+}$* bound to DNA in RMs participates in a Type II mechanism, consistent with our other observations.

Direct observation of $^1O_2$ is possible with emission spectroscopy, because $^1O_2$ luminesces at 1270 nm.[49] We attempted to observe $^1O_2$ luminescence in both buffer and RMs, but no signal was detected even when the reactions were carried out in D_2O. The detection limit of the instrument we used is approximately 300 μM, which means that the steady-state concentration of $^1O_2$ generated in our samples must be below this value. In studies with an intercalating ruthenium complex, quantum yields of $^1O_2$ were determined in the presence of DNA to be 0.26 ± 0.03.[53] In our system, with 50 μM $Ru(bpy)_2dppz^{2+}$ this would mean that the $^1O_2$

Scheme 2. Possible Pathways and Products of G Oxidation in Duplex DNA[a]

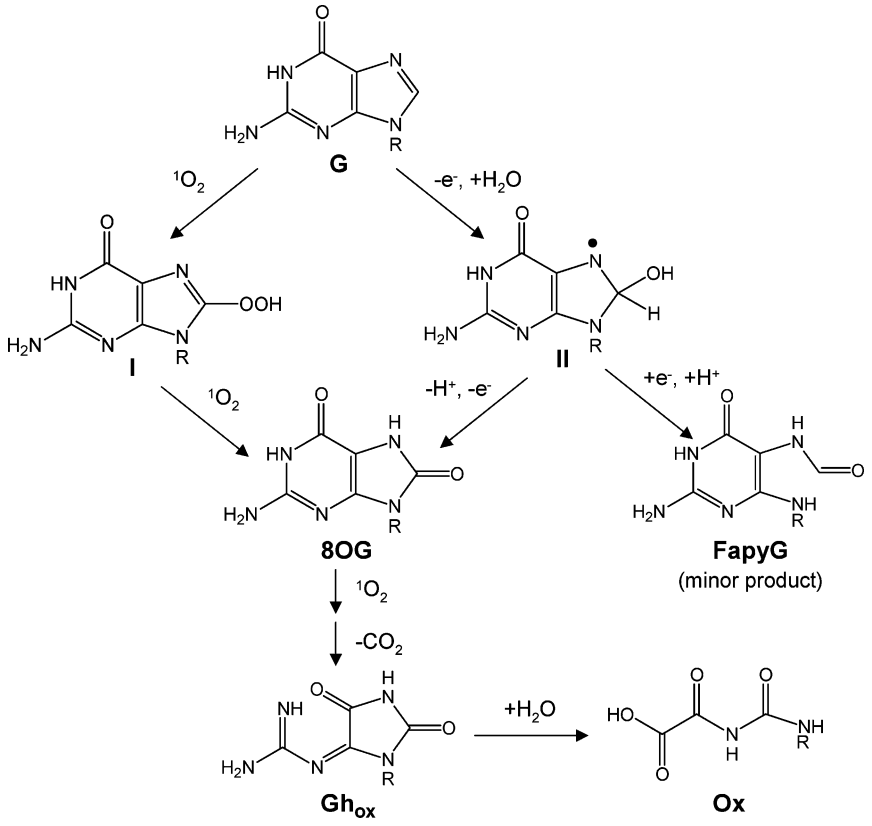

[a] Guanine (G) can be oxidized to form 8-oxo-7,8-dihydroguanine (8OG) via two pathways. Oxidation of G by $^1O_2$ forms an exoperoxide intermediate (I) that reacts with a further equivalent of $^1O_2$ to yield 8OG. Alternatively, one-election oxidation followed by the addition of H_2O generates the reducing radical (II), which upon further oxidation yields 8OG but upon reduction gives 2,6-diamino-4-hydroxy-5-formamidopyrimidine (FapyG). Oxidation of 8OG by $^1O_2$ produces guanidinohydantoin (Gh_{ox}) and oxaluric acid (Ox).

steady-state concentration would be approximately 13 μM, in the absence of $^1O_2$ reaction with DNA. An increase in the concentration of $Ru(bpy)_2dppz^{2+}$ would increase the $^1O_2$ yield, but $Ru(bpy)_2dppz^{2+}$ self-quenches at concentrations >50 μM (Supporting Information, Figure S6). Although we were unable to directly detect $^1O_2$ in the CTAB RMs, we have considerable secondary evidence to support the idea that $^1O_2$ is the DNA oxidant in this system.

Determination of the identity of the G oxidation product generated in RMs is necessary to elucidate the mechanism. As shown in Scheme 2, 8OG is the major product of both one-electron[54] and $^1O_2$ oxidation in duplex DNA;[55] however, 8OG is not piperidine labile,[1] which means that it is not detected on gels like that shown in Figure 5. Further oxidation of 8OG by one-electron oxidants or $^1O_2$ produces piperidine-labile lesions.[1] $IrCl_6^{2-}$ is a one-electron oxidant that oxidizes 8OG but does not oxidize G.[56] Therefore, following treatment with $IrCl_6^{2-}$, piperidine-labile damage observed by denaturing PAGE increases if 8OG is present. When buffer and RM samples without added quencher were treated post-illumination with hexachloroiridate(IV), an increase in piperidine-labile products is observed (Figure 10), indicating that 8OG is produced in both systems. The percent increase in the amount of piperidine-labile lesions after $IrCl_6^{2-}$ treatment is approximately the same in both media, even though the total amounts are not. From these data, we estimate that 5−6% 8OG is present in the RM samples, following a 60 min illumination time.

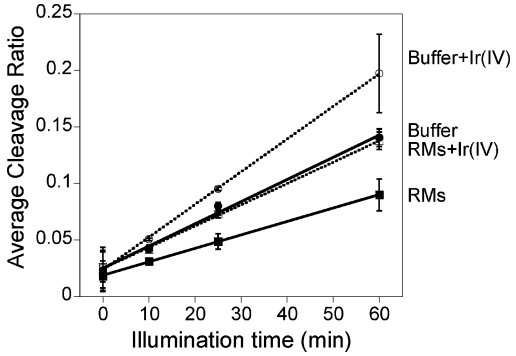

Figure 10. Quantification of average cleavage ratios at G in duplex 21-mer **1**:**2** illuminated in the presence of 50 μM $Ru(bpy)_2dppz^{2+}$ in CTAB RMs (squares) or buffer solution (circles), either untreated (closed symbols) or treated with $IrCl_6^{2-}$ (open symbols).

Because 8OG is a potential product of both direct one-electron and $^1O_2$ oxidation, isotopic labeling studies combined with mass spectrometry were carried out to give further evidence for a $^1O_2$ mechanism in the RMs. RM samples were illuminated in the presence of $H_2{}^{18}O$. If the mechanism is

(53) Hergueta-Bravo, A.; Jimenez-Hernandez, M. E.; Montero, F.; Oliveros, E.; Orellana, G. *J. Phys. Chem. B* **2002**, *106*, 4010.
(54) Spassky, A.; Angelov, D. *Biochemistry* **1997**, *36*, 6571.
(55) Ravanat, J.-L.; Di Mascio, P.; Martinez, G. R.; Medeiros, M. H. G.; Cadet, J. *J. Biol. Chem.* **2001**, *276*, 40601.
(56) Muller, J. G.; Duarte, V.; Hickerson, R. P.; Burrows, C. J. *Nucleic Acids Res.* **1998**, *26*, 2247.

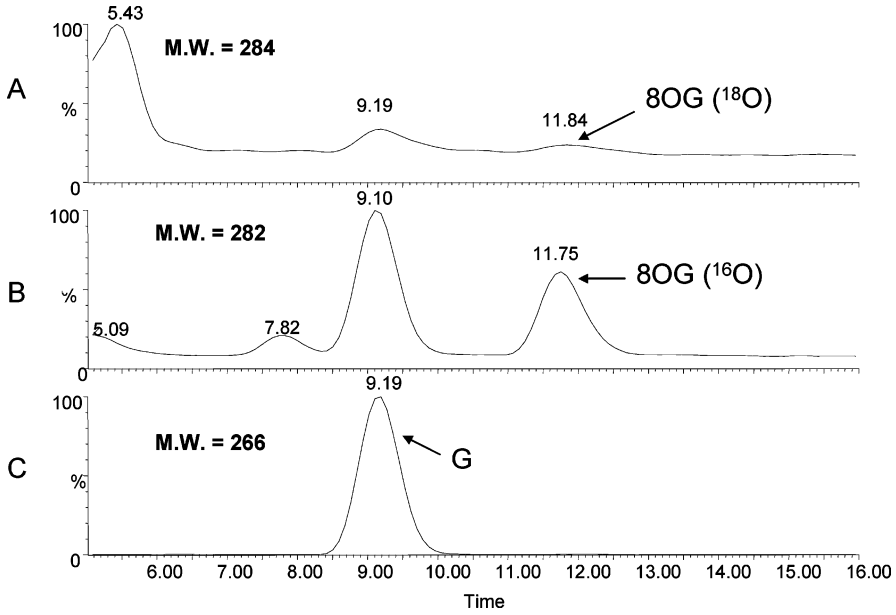

Figure 11. Single-ion LC-MS of an RM sample containing double-stranded 21-mer **1**:**2**, $Ru(bpy)_2dppz^{2+}$, prepared with 95% enriched $H_2{}^{18}O$. Shown are the LC traces for monitoring the presence of (A) 8OG containing ^{18}O (B) 8OG containing ^{16}O and (C) dG.

Table 3. Percent ^{18}O Incorporation into 8OG Generated in RMs Containing 50 μM $Ru(bpy)_2dppz^{2+}$, 10 μM Duplex 21-mer **1**:**2**, and Either Natural Abundance H_2O or 95% Enriched $H_2{}^{18}O$

sample	area G	area 8OG (^{16}O)	area 8OG (^{18}O)	%^{18}O
H_2O	3 490 951	146 757	2792	1.9
$H_2{}^{18}O$	655 786	3400	139	4.1

one-electron oxidation of G by Ru^{3+}, ^{18}O should be incorporated into 8OG in this experiment (Scheme 2). On the other hand, if $^1O_2$ is the oxidant in the system, ^{18}O should not be incorporated into 8OG when $H_2{}^{18}O$ is present. In our samples, only 4% ^{18}O was incorporated into the 8OG (Figure 11 and Table 3), indicating that water is not the source of oxygen atoms in 8OG generated in RMs. These data again support the idea that $^1O_2$ addition to G is the main mechanism in RMs. Approximately 0.5−4% 8OG (relative to G) is produced in the RM samples on the basis of the LC-MS experiments, which is in the same range as the percent 8OG detected using Ir(IV) described above.

The 8OG content in samples affects the levels of piperidine-labile products detected by PAGE. As little as 0.1% 8OG protects G from oxidation by either Type I or one-electron oxidants.[57] The 8OG is preferentially decomposed, thereby shielding G from oxidation.[57] In our system, instead of observing a rapid decrease in the amount of 8OG as a function of reaction time,[57] both buffer and RM samples show an increase in piperidine-labile products post-Ir(IV) treatment, as a function of illumination time. The percent increase in piperidine-labile products generated following Ir(IV) treatment in buffer samples is slightly higher (5−9%) than in RM samples (5−6%). Overall, these data appear to suggest that 8OG is not acting as a sacrificial substrate to screen G from reaction with $^1O_2$ in RMs.

The ability of 8OG to protect G from further oxidation in RMs, however, has not been tested in RMs and depends on the (unknown) rates of reaction between G (or 8OG) and $^1O_2$ in this medium. In organic solvent, the rate constants for the reaction of $^1O_2$ and G or 8OG nucleosides (derivatized so as to be soluble in organic solvent) are 1.36×10^5 and 1.92×10^7 M^{-1} s^{-1}, respectively.[58] These rate constants indicate that 8OG should protect G from reaction with $^1O_2$ (Type II mechanism), but only if the relative magnitudes of these rate constants are maintained in RMs. (Note that the reaction between G or 8OG and $^1O_2$ occurs presumably in the water pools and not in the organic phase of the RM solutions, which means that the rate constants determined in organic solvent cannot be applied directly to the RM system.) At the present time, it is not clear why the 8OG content and the levels of piperidine-labile products detected by PAGE both increase as a function of illumination time. Experiments using mixtures of 8OG- and G-containing oligonucleotides in RMs are planned to explore this issue further.

Taken together, our results indicate that $^1O_2$ is the principal oxidant of G in CTAB RMs containing DNA and $Ru(bpy)_2dppz^{2+}$, even in the presence of oxidative quenchers that generate Ru^{3+}. This result is different than that in buffer solution, where Ru^{3+} oxidation of G is the dominant mechanism in the presence of oxidative quenchers. Thus, there is a shift in the proportion of one-electron versus $^1O_2$-G oxidation chemistry that occurs when $Ru(bpy)_2dppz^{2+}$ is used as the oxidant in RMs. Overall, the yield of piperidine-labile lesions generated by G oxidation in RMs is lower than that in buffer solution, as observed previously in anionic RMs with $Ru(bpy)_3{}^{2+}$.[24] There are several reasons why this may be the case.

First, triplet−triplet annihilation could be occurring to a greater extent in the RM system as a result of an increased proximity of $Ru(bpy)_2dppz^{2+}$* molecules on the DNA. When ruthenium complexes are on average 40 Å apart, their excited

(57) Ravanat, J.; Saint-Pierre, C.; Cadet, J. *J. Am. Chem. Soc.* **2003**, *125*, 2030.

(58) Sheu, C.; Foote, C. S. *J. Am. Chem. Soc.* **1995**, *117*, 6439.

states can interact, which provides a competing decay pathway to either oxidative quenching or $^1O_2$ production.[59] $Ru(bpy)_2dppz^{2+}$ intercalates into B-form DNA approximately every three base pairs in buffer solution,[10] which places the complexes approximately 10 Å apart, and well-within the 40 Å distance associated with triplet−triplet annihilation. In samples without added quencher that are expected to generate $^1O_2$, we observe a decrease in the amount of oxidatively generated damage at G by $Ru(bpy)_2dppz^{2+}$, on going from buffer to RMs (Figure 6). This decrease could be due to a decrease in the average distance between ruthenium complexes in the RMs, which increases triplet−triplet annihilation and produces a corresponding decrease in the amount of $^1O_2$ produced and subsequent DNA oxidation at G (or 8OG). The decrease in the average Ru−Ru distance in RMs could be due to a DNA structural change in the RMs that affects $Ru(bpy)_2dppz^{2+}$ binding.

The RM environment should affect the amount and rate of oxidation reactions when oxidative quenching is used to generate Ru^{3+} because of the proximity of reactants in the RMs. Our Stern−Volmer analysis of the quenching of $Ru(bpy)_2dppz^{2+}$* by $Fe(CN)_6^{3-}$ in the presence of double-stranded DNA shows that $k_q = (1.55 \pm 0.10) \times 10^9$ in buffer and $k_q = (4.98 \pm 0.17) \times 10^9$ M^{-1} s^{-1} in RMs. The close proximity of $Ru(bpy)_2dppz^{2+}$ and $Fe(CN)_6^{3-}$ in RMs leads to a higher quenching constant than in buffer solution. The higher k_q in RMs should lead to an increase in G oxidation by Ru^{3+} in RMs, but that result is not observed. A likely explanation is that back electron transfer (BET) from $Fe(CN)_6^{4-}$ to $Ru(bpy)_2dppz^{3+}$ and/or the G (or 8OG) radical cation is enhanced in the RMs. In other RM systems, the rate of BET increases compared to aqueous solution for the same donor−acceptor pair.[20] Faster BET in the RMs would decrease the amount of piperidine-labile products, even though the rate constant for the oxidative quenching of Ru^{2+}* by $Fe(CN)_6^{3-}$ to produce Ru^{3+} is higher in RMs.

Finally, the switch from the Ru^{3+} oxidation of G to the $^1O_2$ oxidation of G could be because the concentration of molecular oxygen is approximately 10 times higher in the RM solutions than in buffer solution.[60] The rate constant of the reaction between G and $^1O_2$ is approximately[61] 3×10^6 M^{-1} s^{-1}, whereas one-electron transfer from G to various ruthenium polypyridyl oxidants has been measured to occur with a rate constant of up to 1.4×10^7 s^{-1} in buffer solution.[62] These rate constants lead to the prediction that one-electron oxidation and $^1O_2$ oxidation reactions can compete, given that the rates of other reactions (i.e., k_q of O_2 with Ru^{2+}*, triplet−triplet annihilation, and BET) are not known for our system. Our conclusion is that in buffer solution, $Ru(bpy)_2dppz^{2+}$ oxidizes DNA only minimally via $^3O_2$ sensitization, to form $^1O_2$; in contrast, in RMs, $^1O_2$ oxidative modification of G by $Ru(bpy)_2dppz^{2+}$ is favored, even in the presence of oxidative quenchers of Ru^{2+}*.

Because O_2 quenches the $Ru(bpy)_2dppz^{2+}$ excited state to produce $^1O_2$, the higher O_2 concentration in the RM system also is a possible reason for the decrease in emission intensity of $Ru(bpy)_2dppz^{2+}$ in RMs (Figure 1). The resultant decrease in the quantity of excited states also would explain the higher observed k_q in the RMs with $Fe(CN)_6^{3-}$. To probe this possibility, the emission spectra of $Ru(bpy)_2dppz^{2+}$ with herring-testes DNA in buffer and RMs were collected in air and under N_2 (Supporting Information, Figure S7). In buffer solution, the emission intensity of the $Ru(bpy)_2dppz^{2+}$ increased by $13.9 \pm 1.3\%$, and in RMs the emission intensity increased by $20.9 \pm 0.6\%$ when air was excluded from the system. Although the percent increase of the emission intensity is greater in the RMs, it does not fully account for the decrease in emission intensity observed (~30%) for $Ru(bpy)_2dppz^{2+}$ with double-stranded 21-mer in RMs.

Our results further underscore the important role of structure and environment on DNA oxidation.[63] The oxidants and substrates were the same under the two conditions we tested, but by altering the environment of the reaction, the oxidation chemistry changed. The major factors controlling the type of oxidant generated (Ru^{3+} vs $^1O_2$) are related to the unique environment provided by the RMs. The higher concentration of O_2 in the RM solutions could cause $^1O_2$-induced damage at G to effectively compete with one-electron oxidation via Ru^{3+}. In addition, decreases in both emission and induced CD spectra of $Ru(bpy)_2dppz^{2+}$ with double-stranded 21-mer in CTAB RMs suggest a structural change of the DNA in the RM environment. This DNA structural change could affect the number of ruthenium complexes bound to DNA and the rates of the reactions that control the yield of oxidatively generated damage at G. The global environment of the RMs is very different from buffered aqueous solution, but in both media, the initial oxidation step occurs in water. This means that the follow-up chemistry and resulting products of G oxidation should be identical in buffer solution and RMs. Using LC-MS and Ir(IV) treatment, we have shown that 8OG is produced in RMs. However, further work is underway to identify products, in particular FapyG and oxaluric acid, which are produced in the absence or presence of O_2, respectively, and to determine if the yields of these products are sensitive to the change in reaction medium.

(59) Shaw, G. B.; Papanikolas, J. M. *J. Phys. Chem. B* **2002**, *106*, 6156. Ikeda, N.; Yoshimura, A.; Tsushima, M.; Ohno, T. *J. Phys. Chem. A* **2000**, *104*, 6158. Sykora, M.; Kincaid, J. R.; Dutta, P. K.; Castagnola, N. B. *J. Phys. Chem. B* **1999**, *103*, 309.

(60) Murov, S. L.; Carmichael, I.; Hug, G. L. *Handbook of Photochemistry*, 2nd ed.; Marcel Dekker: New York, 1993.

(61) Cadet, J.; Ravanat, J.-L.; Martinez, G. R.; Medeiros, M. H. G.; Di Mascio, P. *Photochem. Photobiol.* **2006**, 1219.

(62) Gutierrez, M. I.; Martinez, C. G.; Garcia-Fresnadillo, D.; Castro, A. M.; Orellana, G.; Braun, A. M.; Oliveros, E. *J. Phys. Chem. A* **2003**, *107*, 3397. Kobayashi, K.; Tagawa, S. *J. Am. Chem. Soc.* **2003**, *125*, 10213.

(63) Delaney, S.; Barton, J. K. *J. Org. Chem.* **2003**, *68*, 6475. Bhattacharya, P. K.; Barton, J. K. *J. Am. Chem. Soc.* **2001**, *123*, 8649. O'Neill, M. A.; Barton, J. K.; Ruba, E.; Hart, J. R.; Williams, T. T.; Dohno, C.; Stemp, E. D.; Delaney, S.; Boon, E. M.; Kisko, J. L.; Pascaly, M.; Bhattacharya, P. K.; Han, K.; Nunez, M. E.; Kelley, S. O.; Hall, D. B.; Lim, A. C.; Arkin, M. R.; Pulver, S. C.; Holmlin, R. E.; Hormann, A.; Olson, E. J.; Barbara, P. F.; Murphy, C. J.; Jenkins, Y.; Friedman, A. E.; Turro, N. J.; Chow, C. S.; Kirsch-De Mesmaeker, A.; Orellana, G. *J. Am. Chem. Soc.* **2004**, *126*, 13234. LaMarr, W. A.; Sandman, K. M.; Reeve, J. N.; Dedon, P. C. *Chem. Res. Toxicol.* **1997**, *10*, 1118. Liang, Q.; Dedon, P. C. *Chem. Res. Toxicol.* **2001**, *14*, 416.

Acknowledgment. This work is supported by an NSF CAREER award to V.A.S. (CHE-0346066). The authors thank Dr. Lisa Kelly and Dr. Sun McMasters for assistance with $^1O_2$ luminescence experiments and Dr. Jim Fishbein and Xuefang Lu for assistance with LC-MS experiments.

Supporting Information Available: Singlet oxygen emission spectrum from C_{60}, Stern−Volmer plots of $Ru(bpy)_2dppz^{2+*}$ quenching by $[Co(NH_3)_5Cl]Cl_2$ and NaN_3, representative gels used to generate plots of average cleavage ratios, self-quenching of $Ru(bpy)_2dppz^{2+}$ in RMs, emission spectra of $Ru(bpy)_2dppz^{2+}$ with/without air in RMs, and LC-MS data for a control sample containing G and 8OG. This material is available free of charge via the Internet at http://pubs.acs.org.

IC0700708